JOURNAL OF SOLID STATE CHEMISTRY 47, 264–277 (1983)

Solid State Studies on Substituted $CuCr_2O_4$ Spinel

K. S. DE,* J. GHOSE, AND K. S. R. C. MURTHY

Department of Chemistry, Indian Institute of Technology, Kharagpur 721302, India

Received June 21, 1982; in revised form November 11, 1982

Changes in crystallographic, electrical, and thermal properties of $CuCr_2O_4$ spinel were investigated by replacing Cu with Mg, i.e., $Cu_{1-x}Mg_xCr_2O_4$, and Cr with Al, i.e., $CuCr_{2-x}Al_xO_4$. The tetragonal distortion in $CuCr_2O_4$ disappeared with 60% replacement of Cu by Mg ($x = 0.6$) or 50% replacement of Cr by Al ($x = 1.0$). The temperature variation of electrical resistivity for all the tetragonal samples was similar to that of $CuCr_2O_4$. The first order, diffusionless phase transition was manifest in the hysteresis loops of log ρ vs $1/T$ plots. The resistivity and activation energy for conduction changed sharply near the phase transition composition. With the replacement of Cr by Al, the conduction in $CuCr_2O_4$ was found to change from p type to n type. The low thermal stability of the spinel was found to be due to a high concentration of tetrahedral Cu^{2+} ions (>80%) and compressed tetragonal distortion which strains the spinel lattice. This strain is removed by replacing either Cu with Mg or Cr with Al, whereby the spinel becomes stable.

A systematic investigation on the catalytic role of transition metal spinel oxides started in the last decade (*1–5*), although their usefulness as catalysts had been recognized long ago. The investigations, so far, have mainly concentrated on the solid state properties of the catalysts, in order to understand the catalytic action of the transition metal ions present in the spinel lattice. A few of the important spinel catalysts have already been extensively studied (*3*), but $CuCr_2O_4$, which is an active catalyst for many important reactions (*6–9*), has not been investigated so far.

The present work was taken up to correlate the solid state and catalytic properties of pure and substituted $CuCr_2O_4$ spinel where the copper and chromium were substituted with the catalytically inert magnesium and aluminium, respectively. The present paper deals with the findings on the effect of these substitutions, as well as substitution of chromium by rhodium and iron, on (i) the spinel structure, (ii) the electrical properties, and (iii) the thermal stability of $CuCr_2O_4$.

Experimental

Preparation of materials. The two series of solid solutions $Cu_{1-x}Mg_xCr_2O_4$ (x = 0, 0.1, 0.2, 0.4, 0.6, 0.8, and 1.0) and $Cu Cr_{2-x}Al_xO_4$ (x = 0.0, 0.1, 0.2, 0.4, 0.6, 0.8, 1.0, 1.2, 1.4, 1.6, 1.8, and 2.0) were prepared by decomposing stoichiometric amounts of metal nitrates at 973 K followed by solid state reaction of the resulting oxides at 1173 K for 24 hr. These solid solutions were also prepared by coprecipitating metal ions as hydroxides, with ammonia, at 353 K with subsequent calcination of the precipitate. The precipitation was carried

* To whom correspondence should be addressed.

0022-4596/83 $3.00

out at 11 pH for Mg substituted solid solutions and calcined at 973 K for 6 hr, while for Al substituted solid solutions the precipitation was carried out at 6.5 pH and calcined at 1073 K for 24 hr. In all the preparations completion of precipitation was ensured by testing the supernatant liquid.

$CuRh_2O_4$ and $CuRh_{0.1}Cr_{1.9}O_4$ were prepared by impregnating stoichiometric amounts of Rh_2O_3 with cupric and chromium nitrate solution for 24 hr and then decomposing the nitrates at 973 K. The resulting oxides were pressed into pellets under a pressure of 10 ton/cm^2, and were fired at 1223 K for 60 hr. To prevent the formation of $Cu_2Cr_2O_4$ and $Cu_2Rh_2O_4$ (*10, 11*), all the chromium rich samples ($CuCr_2O_4$ – $MgCr_2O_4$ and $CuCr_{1.8}Al_{0.2}O_4$ – $CuCrAlO_4$) and the rhodium samples ($CuRh_2O_4$, $CuRh_{0.1}Cr_{1.9}O_4$) were finally annealed at 973 K for 24 hr.

$CuFe_2O_4$ was prepared by decomposing the metal nitrates at 973 K followed by solid state reaction at 1173 K for 24 hr.

After the final heat treatment, all the samples were slowly cooled to room temperature at a rate of 2°/min.

X-ray diffraction studies. X-ray diffraction analysis of all the products was carried out using the Debye–Scherrer powder technique with a Philips X-ray diffraction unit model PW 1012/10. For chromium-rich samples a chromium target was used with vanadium filter, while for copper-rich samples a copper target with nickel filter was used.

Lattice parameters of tetragonal phases were determined with Hull's charts for tetragonal structures while those of cubic samples were determined by extrapolation in the coordinates of a vs $\mathrm{Cos}^2\theta$ ($1/\theta + 1/\mathrm{Sin}^2\theta$) where a is the lattice parameter calculated from the reflections whose Bragg angle is θ. The cation distribution in $Cu Cr_{2-x}Al_xO_4$ was determined from the intensities of 220, 311, 400, 422 lines, following the method of Porta *et al.* (*12*).

Electrical resistivity measurements. Samples were pressed into pellets under a pressure of 10 tons/cm^2, and were annealed in air at 873 K for several hours. Resistivity of these pellets was determined in air between 373 and 923 K, using a two-probe technique (*13*).

Thermoelectric power. Thermoelectric power of all the samples was determined qualitatively at 423 K. The sample pellet was clamped between two stainless steel electrodes and a temperature gradient of approximately 25° was maintained across the pellet. A galvanometer (Leeds & Northrup Co., model 2239) with lamp and scale arrangement was used to measure the deflection.

Thermal studies. High temperature X-ray diffraction patterns of all the tetragonal samples were taken using a Philips X-ray diffractometer model MRC, X-86-N3, provided with high temperature attachment.

The thermal stability of all the compounds prepared, was determined by the following method: known amounts of samples were kept at 1300 K in an alumina boat for 10 hr in air, and subsequently quenched and cooled in a dessicator. The percentage weight loss was determined gravimetrically and the resulting products were analyzed by X-ray diffraction.

Results

X-ray diffraction patterns of $CuCr_2O_4$, $CuFe_2O_4$, $CuRh_2O_4$, $CuCr_{1.9}Rh_{0.1}O_4$, and the solid solution samples $Cu_{1-x}Mg_xCr_2O_4$, $CuCr_{2-x}Al_xO_4$ show them to be single phase spinels. Figure 1a shows the variation of both, lattice parameters, and the cube root of unit cell volume, with composition for $Cu_{1-x}Mg_xCr_2O_4$. The change in tetragonal distortion with increasing concentration of magnesium is shown in Fig. 1b. Figure 2a and b give the corresponding plots for $Cu Cr_{2-x}Al_xO_4$. The plot of the tetragonal to cubic phase transition temperature T_t for all

the tetragonal solid solution samples, against the degree of tetragonality, is shown in Fig. 3. The change in tetrahedral copper concentration with increasing aluminium content, in $CuCr_{2-x}Al_xO_4$, is given in Fig. 4. Figure 5 shows the change in tetragonality with change in the tetrahedral copper concentration for $Cu_{1-x}Mg_xCr_2O_4$, $CuCr_{2-x}Al_xO_4$, $CuRh_{2-x}Fe_xO_4$, and $CuCr_{2-x}Fe_xO_4$. The data for the latter two systems have been taken from references (*10*) and (*23*).

The log ρ vs $1/T$ plots for all the solid solution samples with cubic structure, show linearity in the measured temperature range, as found with the end member spinels. The tetragonal samples also show similar results, except that at certain temperatures nonlinearity is observed. The log resistivity vs $1/T$ plots of all the tetragonal samples are shown in Fig. 6a–f. The changes in activation energy for electrical conduction q and log resistivity, with composition x of the solid solution $Cu_{1-x}Mg_xCr_2O_4$ samples at 473 K, are shown in Fig. 7. Corresponding plots for $CuCr_2O_4$–$CuAl_2O_4$ are given in Fig. 8.

The apparent distance between two adjacent octahedral metal ions (B–B distance) as well as type of conduction in the various $Cu_{1-x}Mg_xCr_2O_4$ and $CuCr_{2-x}Al_xO_4$ samples is given in Tables I and II, respectively. Table II also gives the fraction of copper, aluminium, and chromium on B sites in these samples. Table III gives the phases present in the samples $Cu_{1-x}Mg_xCr_2O_4$, $CuCr_{2-x}Al_xO_4$ prepared by coprecipitation, $CuRh_2O_4$, and $CuFe_2O_4$ after the heat treatment. The percentage weight loss after the heat treatment is also given in Table III.

Discussion

The present studies were carried out with solid solution samples prepared by decomposition of nitrates followed by solid state reaction, as well as coprecipitation and calcination, because there is some controversy in the literature (*14, 15*) about the dependence of structural distortion on the method of preparation.

X-Ray Diffraction

X-ray patterns show that irrespective of the method of preparation, all the spinel samples obtained by decomposition of nitrates and solid state reaction differ very little in their lattice parameters from the corresponding spinels obtained by coprecipitation.

Figure 1a shows that the tetragonal distortion in $Cu_{1-x}Mg_xCr_2O_4$ decreases linearly as x changes from 0 to 0.4, but between 0.4 to 0.6 the decrease is rather sharp. In case of $CuCr_{2-x}Al_xO_4$ (Fig. 2a) the decrease in distortion as x changes from 0 to 0.8 is comparatively small and only before the disappearance of distortion is the decrease sharp. However, the tetragonal to cubic phase transition temperature (Fig. 3), varies linearly with the degree of tetragonality in both the systems, as observed in the manganate spinel systems (*16*). In both the solid solutions studied, near the tetragonal to cubic phase transition, a small anomaly is observed in the straight line plot of $V^{1/3}$ (cube root of unit cell volume) against composition. This anomaly may be attributed to the first order nature of the tetragonal to cubic phase transition (*17*).

The plots of Fig. 1a and b show that when about 60% of the Cu in $CuCr_2O_4$ is replaced by Mg, the spinel becomes cubic, which is well in agreement with the values reported by Delorme (*14a*) and Ustyantsev *et al.* (*14b*), but different from that reported by Yureva *et al.* (*15*). For $CuCr_{2-x}Al_xO_4$ system the results in Fig. 2a and b show that when 50% of Cr is replaced by Al ($x = 1$ or $CuCrAlO_4$), the distortion in $CuCr_2O_4$ disappears. This critical concentration of Cr below which the distortion disappears, however, differs from the values reported earlier (*14*).

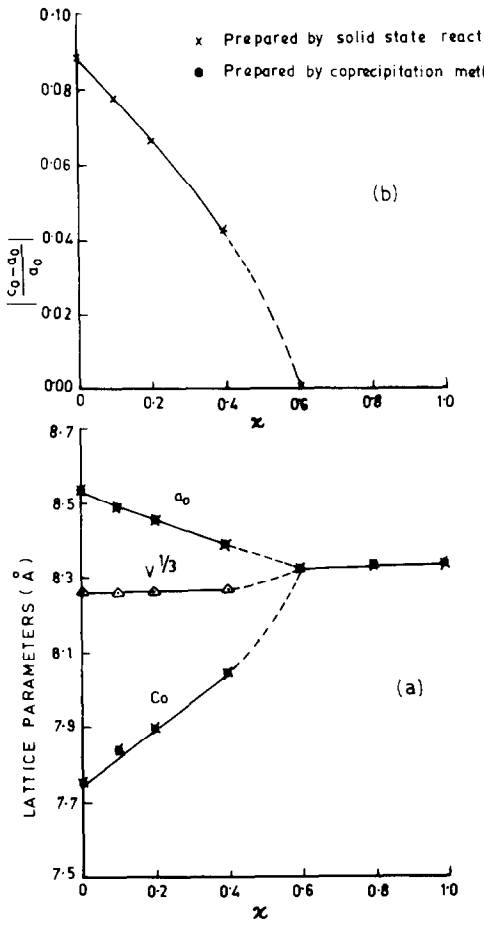

FIG. 1. Variation in lattice parameters, cube root of unit cell volume (a), degree of tetragonality (b) with composition x for $Cu_{1-x}Mg_xCr_2O_4$. (Dashed lines indicate the composition range in which the cubic phase appears and coexists with the tetragonal phase.)

Cr^{3+} has the highest octahedral site preference energy and hence both $CuCr_2O_4$ and $MgCr_2O_4$ are normal spinels (*18*). Thus the cation distribution in the solid solution $Cu_{1-x}Mg_xCr_2O_4$ may be assumed to remain normal, i.e., Mg is expected to replace Cu on tetrahedral sites (*A* sites) without disturbing the cation occupancy of octahedral sites (*B* sites). However, in case of $CuCr_{2-x}Al_xO_4$ the cation distribution is expected to change from normal to random with increasing x as the octahedral site preference energies of both Cu^{2+} and Al^{3+} are comparable (Cu^{2+}: −9.4 kcal/mole, Al^{3+}: −10.0 kcal/mole) (*18*). Thus, Al substitution for octahedral Cr will subsequently lead to a redistribution of copper and aluminium on the tetrahedral and octahedral sites. This is evident in Fig. 4, where it is shown that as x increases from 0 to 2, the fraction of *A* site copper decreases linearly from 1.0 to 0.56. A comparison of Figs. 2 and 4 reveals that when about 20% of *A* site copper is transferred to octahedral sites, the spinel becomes cubic. Hence it appears that irrespective of whether tetrahedral Cu or octahedral Cr is replaced by other ions, a definite amount of copper on the tetrahedral sites, i.e., a critical concentration, is required for structural distortion. However, the critical concentration of tetrahedral copper, required for distortion may not be the same for all spinel compounds, which is clearly shown in Fig. 5. It is evident from the figure that this critical concentration is high for $CuCr_{2-x}Al_xO_4$, $CuCr_{2-x}Fe_xO_4$, and $CuRh_{2-x}Fe_xO_4$ as compared to $Cu_{1-x}Mg_xCr_2O_4$ which has no copper on the octahedral sites. Thus, a higher value of the critical concentration for compounds having octahedral copper suggests the possibility of a compensation effect of octahedral copper on the tetragonal distortion due to tetrahedral copper, in the partially inverse spinels. This is probably because Cu^{2+} ions on *B* sites tend to elongate the surrounding octahedra in contrast to the compression affected by *A* site Cu^{2+} ions (*19, 20*). Furthermore, the magnitude of the compensation effect is expected to vary from compound to compound as the elongated distortion due to *B* site Cu^{2+} ions is considerably influenced by the presence of other non Jahn–Teller active ions (*21, 22*). Thus, in $CuCr_{2-x}Fe_xO_4$, $CuCr_{2-x}Al_xO_4$, and $CuRh_{2-x}Fe_xO_4$ systems, the non J–T active ions are Cr^{3+}, Fe^{3+}, Al^{3+}, and Rh^{3+} which will indirectly affect the critical concentration of *A* site Cu^{2+} ions, and hence

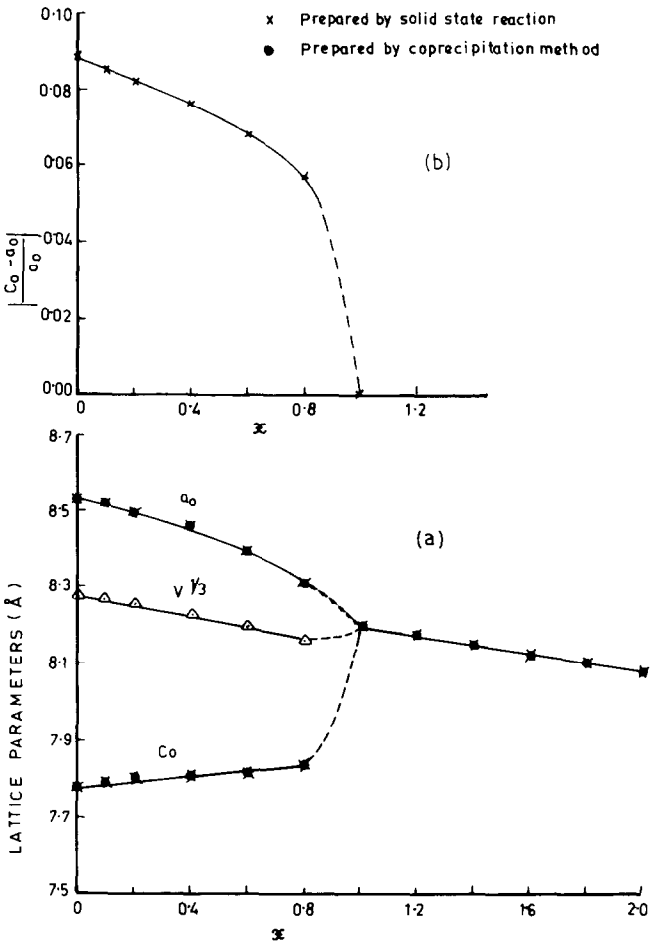

FIG. 2. Variation in lattice parameters, cube root of unit cell volume (a), degree of tetragonality (b) with x for $CuCr_{2-x}Al_xO_4$.

for $CuCr_{2-x}Fe_xO_4$ a value of 0.65 is reported (*10*) while a value of 0.775 has been found for $CuCr_{2-x}Al_xO_4$, which is similar to the value reported for $CuRh_{2-x}Fe_xO_4$ (*23*). Moreover, it is evident from Fig. 5, that up to a decrease of about 0.85 in the concentrations of *A* site copper the change in distortion is almost the same for all the solid solutions. But with further decrease, the change varies differently for the four samples and a sharp decrease in distortion occurs for a change from 0.825 to 0.775 for $CuCr_{2-x}Al_xO_4$ and $CuRh_{2-x}Fe_xO_4$ and from 0.765 to 0.65 for $CuCr_{2-x}Fe_xO_4$. For $Cu_{1-x}Mg_xCr_2O_4$, however, the decrease is quite gradual. From these results it may be concluded that the elongated distortion by *B* site Cu^{2+} ions is not stabilized until a certain concentration of *B* site Cu^{2+} ions is present and this value is approximately 0.17 for $CuCr_{2-x}Al_xO_4$ and $CuRh_{2-x}Fe_xO_4$ and 0.24 for $CuCr_{2-x}Fe_xO_4$. The absence of this compensation effect in $Cu_{1-x}Mg_xCr_2O_4$ is understandable as no Cu^{2+} ions are present on the octahedral sites of any of these solid solution samples.

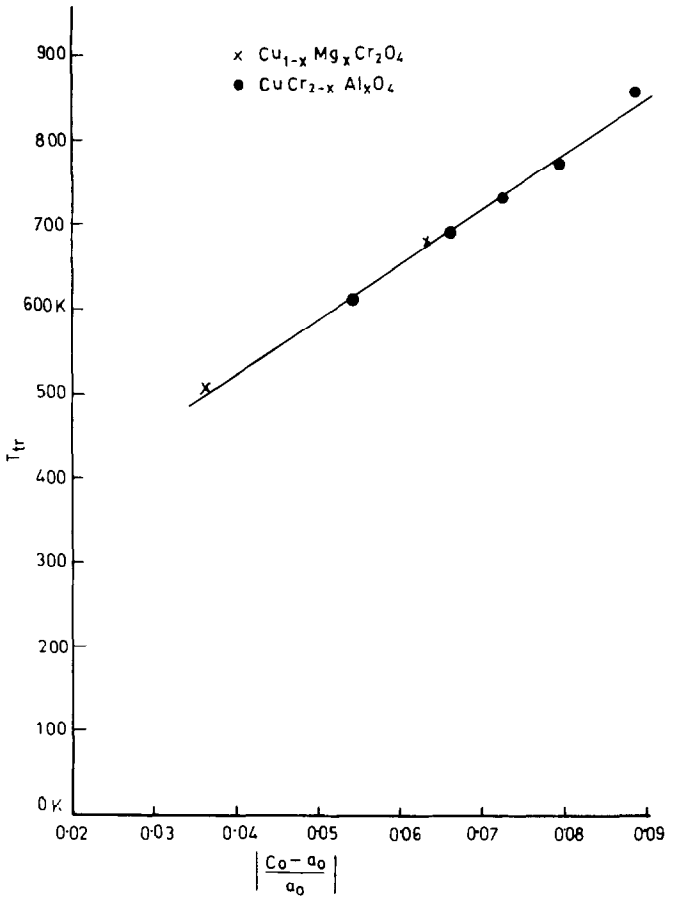

FIG. 3. Dependence of tetragonal to cubic phase transition temperature on degree of tetragonality.

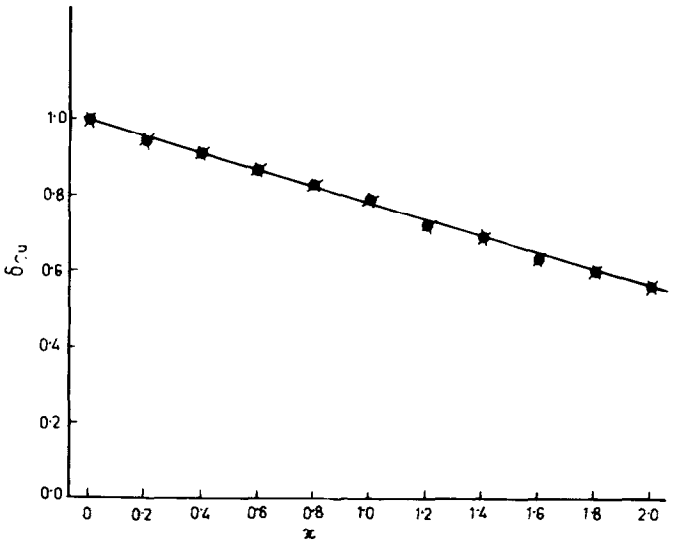

FIG. 4. Change in δ, fraction of tetrahedral copper, with x for $CuCr_{2-x}Al_xO_4$.

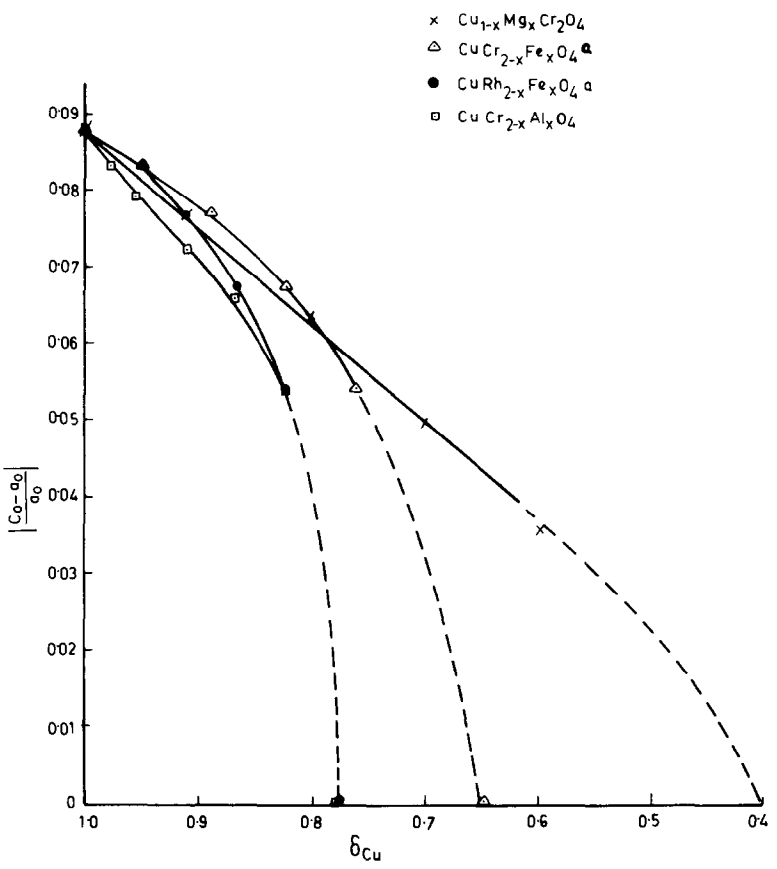

FIG. 5. Change in tetragonality with tetrahedral copper concentration for $Cu_{1-x}Mg_xCr_2O_4$, $CuCr_{2-x}Al_xO_4$, $CuRh_{2-x}Fe_xO_4$, and $CuCr_{2-x}Fe_xO_4$, (a) data taken from Refs. (*10*) and (*23*).

Electrical Resistivity

The results show that in the substituted tetragonal samples, the change in resistivity with temperature, while heating and cooling, is similar to those observed for $CuCr_2O_4$, reported earlier (*13*). Thus, the resistivity plots in Fig. 6a–f show a change in slope in the heating curve due to tetragonal to cubic phase change and on cooling the reverse transition occurs. The tetragonal to cubic phase transition is also confirmed by high temperature X-ray, which showed the presence of only cubic phase at higher temperatures. Furthermore, the phase transition is diffusionless and of the first order as shown by the presence of the hysteresis loops in the heating and cooling plots.

Conduction in these solid solutions may be due to hopping of charge carriers among octahedral site cations, as has been found in the case of $CuCr_2O_4$. Thus, no change in either q or ρ should be expected when the octahedral Cr^{3+} concentration remains constant while tetrahedral Cu is progressively replaced by Mg, for all values of x in $Cu_{1-x}Mg_xCr_2O_4$. But, contrary to expectations, results in Fig. 7, show an increase in activation energy and $\log \rho$ between $x = 0.4$ and 0.6 which happens to be the composition range where the spinel undergoes a tetragonal to cubic phase transition.

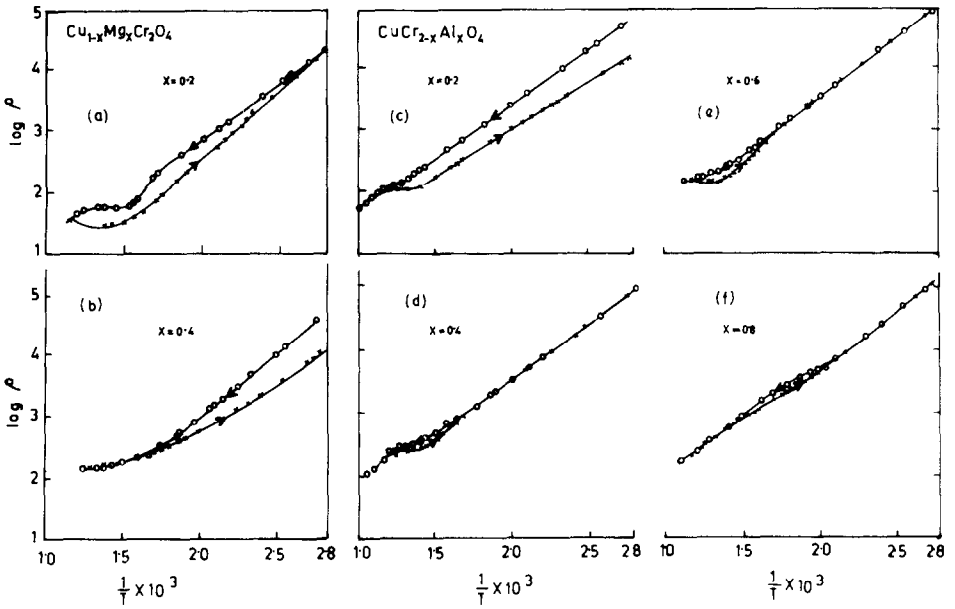

FIG. 6. Log-specific resistivity versus reciprocal of absolute temperature for $Cu_{0.8}Mg_{0.2}Cr_2O_4$ (a), $Cu_{0.6}Mg_{0.4}Cr_2O_4$ (b), $CuCr_{1.8}Al_{0.2}O_4$ (c), $CuCr_{1.6}Al_{0.4}O_4$ (d), $CuCr_{1.4}Al_{0.6}O_4$ (e), $CuCr_{1.2}Al_{0.8}O_4$ (f) in air.

Such anomalies in the composition vs q curves have been observed earlier in other cooperative Jahn–Teller distorted spinel systems (*24*), but the precise nature of the bulk distortion on resistivity and q has not been investigated. Table I shows that a change in distortion is accompanied with a change in the cation–cation distance, which could alter the activation energy, as the activation energy for electron hopping is sensitive to the distance between cations participating in the hopping process (*17, 25*). It

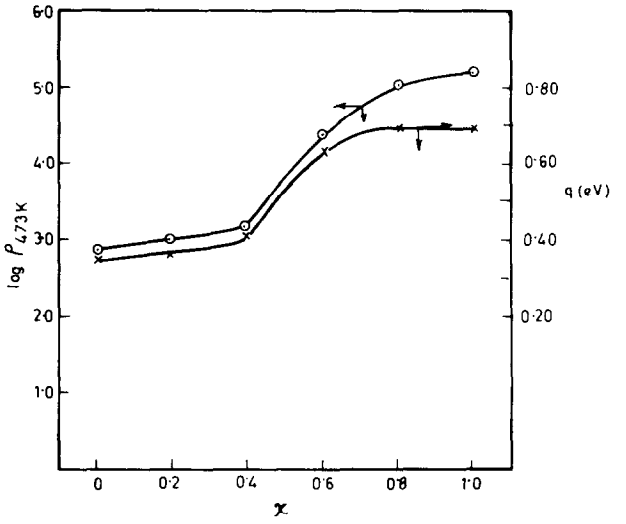

FIG. 7. Variation in activation energy, Log-resistivity at 473 K, with x for $Cu_{1-x}Mg_xCr_2O_4$.

TABLE I

VARIATION IN APPARENT B–B DISTANCE, c_0/a_0 RATIO AND TYPE OF CONDUCTION, WITH x, IN THE $Cu_{1-x}Mg_xCr_2O_4$ SYSTEM

Sample	B–B distance in Å (±0.003)	c_0/a_0	Type of conduction
$CuCr_2O_4$	2.922	0.912	p type
$Cu_{0.8}Mg_{0.2}Cr_2O_4$	2.918	0.934	p type
$Cu_{0.6}Mg_{0.4}Cr_2O_4$	2.920	0.958	p type
$Cu_{0.4}Mg_{0.6}Cr_2O_4$	2.941	1.000	p type
$Cu_{0.2}Mg_{0.8}Cr_2O_4$	2.945	1.000	p type
$MgCr_2O_4$	2.945	1.000	p type

is apparent from Table I that the variation in B–B distance is almost negligible in the composition range $x = 0$ to 0.4, but increases perceptibly between 0.4 and 0.6, and thereafter remains almost constant for higher values of x. From this it may be concluded that a change in cation–cation separation associated with distortion leads to the observed variation in q and log ρ.

Unlike $Cu_{1-x}Mg_xCr_2O_4$, the concentration of octahedral Cr constantly decreases in $CuCr_{2-x}Al_xO_4$ solid solutions and with the introduction of Al, the fraction of Cu and Al on B sites increases. These changes are likely to affect the conduction mechanism of $CuCr_2O_4$. Thus when all the three cations, Cu, Cr, and Al, are present, the following contributions towards conduction may be expected, due to electron hopping in the octahedral sites between

(i) Cr–Cr
(ii) Cu–Cr
(iii) Cu–Cu
(iv) Cr–Cu–Cr
(v) Cu–Cr–Cu
(vi) Cr–Al–Cr
(vii) Cu–Al–Cu

and also electron hopping between the three cations. However, some of these will be dominating the conduction mechanism, depending on the relative concentrations of the cations on the B sites.

According to Pomonis and Vickerman (*3*), when a charge carrier hops over a non-transition-metal ion like Al^{3+}, the process involves high activation energy. Thus conduction by (vi) and (vii) should involve high activation energies and become dominant only when the concentration of Cr and Cu are small. But none of the solid solutions studied have low concentration of both Cu and Cr at the same time and hence it appears that dominant contributions will be from (i) to (v). Again, in chromium rich samples, contribution from (i) will always be the most dominant, for it involves direct hopping via t_{2g} orbitals of Cr ions. In (ii) to (v) the hopping involves e_g orbitals of Cu ions and thus will only occur via the oxide ion p orbitals which in effect is indirect hopping.

It is evident from Table II that with increasing x in a particular phase, the B–B distance gradually decreases. This trend, however, breaks at the tetragonal to cubic phase transition but again continues with the cubic phase. With a decrease in the B–B distance it is expected that activation energy will decrease, but Fig. 8 shows that q does not change much with x except at $x = 0.2$ and 1.0. The initial increase in q up to $x = 0.2$ may be attributed to the introduction of small amounts of Cu and Al to the octahedral sites, leading to the onset of mechanisms (ii) and (vii) and a decrease in the contribution from Cr–Cr direct hopping. This will cause the observed increase in activation energy as well as resistivity. Moreover, the thermoelectric power measurements reveal that with the introduction of a small amount of Al in the spinel lattice, $CuCr_2O_4$ changes from p type to an n type semiconductor and this could also be responsible for the observed increase in q.

Table II shows that with further increase in x, B–B distance decreases, i.e., Cr ions come closer to each other, which should

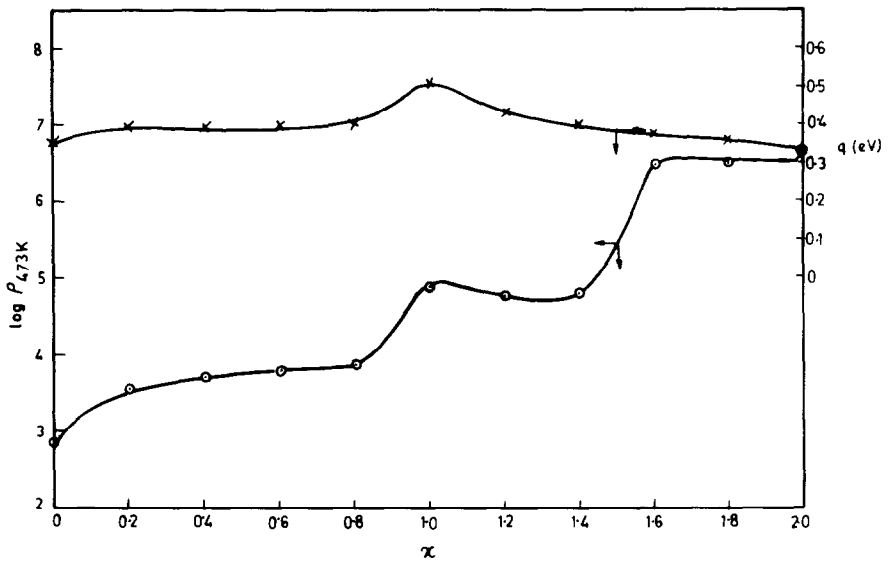

FIG. 8. Variation in activation energy, Log-resistivity at 473 K, with x for $CuCr_{2-x}Al_xO_4$.

again decrease the overall activation energy. However, a simultaneous increase in the Al concentration will tend to compensate this decrease in activation energy. Furthermore, with the introduction of Al, some Cu ions will migrate to the *B* sites, which is likely to have some effect on the magnitude of activation energy. Thus, it appears that all these together seem to have a net effect of keeping the activation energy almost constant for all values of x above 0.2 except at $x = 1.0$. The increase in q at $x = 1.0$ may be attributed to the tetragonal to cubic phase transition leading to a sudden change in *B–B* distance (Table II).

The change in resistivity is similar to the

TABLE II

VARIATION IN APPARENT *B–B* DISTANCE, c_0/a_0, OCTAHEDRAL CONCENTRATIONS OF Cu, Cr, Al AND TYPE OF CONDUCTION, WITH x, IN THE $CuCr_{2-x}Al_xO_4$ SYSTEM

Sample	*B–B* distance in Å (±0.003)	c_0/a_0	Fraction of metal ions on *B* sites			Type of conduction
			Cu	Al	Cr	
$CuCr_2O_4$	2.924	0.912	0	0	2.0	*p* type
$CuCr_{1.8}Al_{0.2}O_4$	2.918	0.918	0.06	0.14	1.8	*n* type
$CuCr_{1.6}Al_{0.4}O_4$	2.906	0.924	0.09	0.31	1.6	*n* type
$CuCr_{1.4}Al_{0.6}O_4$	2.895	0.932	0.13	0.47	1.4	*n* type
$CuCr_{1.2}Al_{0.8}O_4$	2.883	0.943	0.18	0.62	1.2	*n* type
$CuCrAlO_4$	2.896	1.000	0.22	0.78	1.0	*n* type
$CuCr_{0.8}Al_{1.2}O_4$	2.889	1.000	0.27	0.93	0.8	*n* type
$CuCr_{0.6}Al_{1.4}O_4$	2.880	1.000	0.31	1.09	0.6	*n* type
$CuCr_{0.4}Al_{1.6}O_4$	2.871	1.000	0.35	1.25	0.4	*n* type
$CuCr_{0.2}Al_{1.8}O_4$	2.864	1.000	0.39	1.41	0.2	*n* type
$CuAl_2O_4$	2.857	1.000	0.44	1.56	0.0	*n* type

changes in q up to $x = 1.0$. For higher values of x, resistivity remains almost constant up to $x = 1.4$, whereby it suddenly increases by almost $1\frac{1}{2}$ orders of magnitude at $x = 1.6$. At this composition the interaction between Cr ions appears to be negligible (*3*) since Cr ions are quite separated and the probability of direct hopping between Cr ions becomes small. Between $x = 1.6$ to 2.0, octahedral sites are occupied by sufficient number of Cu ions (0.35–0.44) to establish a considerable Cu–Cu interaction. Hence for higher values of x ($x > 1.6$), the major contribution towards total conductivity would be Cu–Cu hopping which involves transfer of an e_g electron via oxide ion orbitals, and the observed high resistivity in this region may then be due to the low mobilities associated with such hopping.

Studies on thermoelectric power of the solid solution samples (Tables I and II) reveal that $CuCr_2O_4$ is a p type semiconductor and when Cu is replaced by Mg, the nature of conduction does not change. But even for a small replacement of Cr by Al in $CuCr_{2-x}Al_xO_4$, the spinel changes to an n type semiconductor. Replacement of Cr by Rh, however, does not bring about such a change and even when all the Cr is replaced by Rh, i.e., $CuRh_2O_4$, the semiconductor remains p type. The only difference between these two substitutions is that introduction of Al changes the cation distribution of normal $CuCr_2O_4$ with some Cu ions migrating to the octahedral sites whereas, Rh, having almost a similar preference for the octahedral site as Cr, prevents any such migration whereby Cu ions are forced to remain on the tetrahedral sites of the spinel (*23*). Thus it appears that the presence of even a small amount of Cu ions on B sites strongly modify the electrical properties of $CuCr_2O_4$ spinel.

Thermal Stability

Thermal studies on $CuCr_2O_4$ (*26, 27*) have earlier shown that the spinel is unstable at temperatures above 1173 K, decomposing into $Cu_2Cr_2O_4$ and Cr_2O_3. Extensive studies (*28*) have been carried out on the decomposition of $CuCr_2O_4$ and the thermodynamic studies by Navrotsky *et al.* (*29*) and Muller *et al.* (*30*) reveal that $CuCr_2O_4$ is comparatively less stable among the $3d$ transition metal chromites and also among other Cu containing oxide spinels.

Results in Table III show that the thermal instability of $CuCr_2O_4$ persists even when 20% of Cu is replaced by Mg or 30% of Cr is replaced by Al. However, with further replacements, the spinel phase becomes stable. This improvement in stability is likely to depend on the changes in cation distribution associated with the substitution of the cations of $CuCr_2O_4$ by other ions, as well as change in the lattice parameters of the spinel.

In $Cu_{1-x}Mg_xCr_2O_4$, since Mg progressively replaces tetrahedral Cu without disturbing the octahedral Cr, any change in thermal stability in this system, with increasing x, should be a function of the amount of the tetrahedral Cu only. The results show that the thermal stability increases only after 20% of A site Cu is replaced by Mg and with 40% replacement a completely stable spinel is formed. The stability increase is also accompanied by a 25% decrease in the tetragonal distortion (Fig. 1b). From Fig. 2b and Table III it is evident that in $CrCr_{2-x}Al_xO_4$ system, thermal stability increases with 30% replacement of Cr by Al which actually leads to a 15% decrease in the concentration of A site Cu. Again, similar to $Cu_{1-x}Mg_xCr_2O_4$, the increase in thermal stability, in this system also, is accompanied by a 25% decrease in the tetragonal distortion. Thus, increase in the thermal stability of $CuCr_2O_4$ seems to be always accompanied by a decrease in both A site Cu concentration ($\simeq$15–20%) as well as tetragonal distortion ($\simeq$25%) of the spinel. Hence it may be concluded that the thermal instability of $CuCr_2O_4$ is due to the

TABLE III

% WEIGHT LOSS AND PHASES PRESENT IN VARIOUS SPINEL SAMPLES AFTER HIGH TEMPERATURE TREATMENT

Sample no.	Spinel system	Composition	Weight loss %	Phases present
1.	$Cu_{1-x}Mg_xCr_2O_4$	$x = 0$	3.5	$Cu_2Cr_2O_4$, Cr_2O_3, and $CuCr_2O_4$
		0.1	3	$Cu_2Cr_2O_4$, Cr_2O_3, and spinel phase
		0.2	1.5	Traces of $Cu_2Cr_2O_4$, Cr_2O_3, and spinel phase
		0.4–1.0	0.8–0.9	Spinel phase
2.	$CuCr_{2-x}Al_xO_4$	$x = 0.1$	2.9	$Cu_2Cr_2O_4$, Cr_2O_3, and spinel phase
		0.2	2.5	$Cu_2Cr_2O_4$, Cr_2O_3, and spinel phase
		0.4	1.9	$Cu_2Cr_2O_4$, Cr_2O_3, and spinel phase
		0.6	1.5	Traces of $Cu_2Cr_2O_4$ and Cr_2O_3 and spinel phase
		0.8–2.0	0.8–0.7	Spinel phase
3.	$CuRh_2O_4$	—	—	$Cu_2Rh_2O_4$, Rh_2O_3 and $CuRh_2O_4$
4.	$CuFe_2O_4$	—	—	Spinel phase

presence of more than 80% Cu on the tetrahedral sites and the relative decrease or increase in the amount of Cr with respect to tetrahedral Cu, has very little influence on the stability of $CuCr_2O_4$. This is also supported by the thermal instability found for normal $CuRh_2O_4$, where all the octahedral Cr is replaced by octahedral Rh (Table III). However, Cr seems to have some indirect influence on the thermal instability of the spinel: due to its strong preference for the octahedral sites, Cr^{3+} ions prevent the migration of Cu^{2+} ions from *A* sites to *B* sites even at high temperatures, whereby there is always a large concentration of Cu on the tetrahedral sites.

Along with the Cu concentration on the *A* sites, thermal instability is also associated with tetragonal distortion. To determine the exact role of distortion, studies on $CuFe_2O_4$ were also carried out. This spinel has an elongated distortion with $c/a > 1$ as compared to a compressed distortion ($c/a < 1$) of $CuCr_2O_4$. The results in Table III show that unlike $CuCr_2O_4$, this spinel is thermally stable up to 1300 K. Detailed studies (*31, 32*) on the two compounds have shown that the distortion in $CuCr_2O_4$ affects the tetrahedral angles, whereas, in $CuFe_2O_4$, the distortion affects the Cu–O distances resulting in four short Cu–O distances lying in a plane, and two long Cu–O distances perpendicular to this plane. Thus, it seems that the thermal instability in $CuCr_2O_4$ arises partly due to this effect of distortion on the spinel structure. As the distortion leads to $c/a < 1$, i.e., compression along the *c* axis, with no change in Cu–O distances, the spinel is under strain which becomes considerable when more than 80% of Cu^{2+} ions are on the tetrahedral sites, thereby making $CuCr_2O_4$ thermally unstable. Thus

removal of about 20% of Cu^{2+} ions from the tetrahedral sites is required to ease this strain and make a thermally stable spinel.

Conclusions

From the above studies it may be concluded that most of the interesting solid state properties of $CuCr_2O_4$ arise due to the presence of a critical concentration of ($\simeq$ 80%) Jahn–Teller active Cu^{2+} ions exclusively on the tetrahedral sites and the strong preference of Cr^{3+} ions for the octahedral sites.

Thus, the crystallographic studies show that the compressed tetragonal distortion disppears when the concentration of Cu^{2+} ions on the *A* sites is below the critical concentration. However, it has also been found that the *A* site distortion can be compensated for by the presence of a certain concentration (20%) of *B* site Cu^{2+} ions as the latter leads to an elongated distortion. Electrical studies also show that substitution of chromium by an ion having not so strong a preference for the octahedral sites, leads to a change in the electrical properties of the spinel, probably due to the presence of copper on the octahedral sites. Finally, the thermal studies show that the unusual thermal instability of $CuCr_2O_4$ is again due to large concentrations (>80%) of Cu ions on *A* sites, which, along with a compressed distortion along the *c* axis give rise to a strain in the crystal structure. Thus by decreasing the *A* site Cu ion concentration the strain can be eased and the thermal stability of the spinel may be improved. Cr ions seem to have only an indirect influence on the instability of the spinel, and this is due to its strong preference for *B* sites which always leads to a large concentration of Cu ions on *A* sites.

Further investigation on the catalytic activity of these substituted $CuCr_2O_4$ samples, having such interesting solid state properties, is in progress.

Acknowledgments

The authors thank the Chemistry Division, Bhabha Atomic Research Centre, Bombay, India for their help with high temperature X-ray diffraction studies.

References

1. J. C. VICKERMAN, *Trans. Faraday Soc.* **67,** 665 (1971).
2. A. CIMINO AND M. SCHIAVELLO, *J. Catal.* **20,** 202 (1971).
3. P. POMONIS AND J. C. VICKERMAN, *J. Catal.* **55,** 88 (1978).
4. G. K. BORESKOV, *in* "Proc. 5th Inter. Congr. Cat." (Hightower, Ed.), p. 981, North-Holland, Amsterdam (1973).
5. R. J. RENNARD AND W. L. KEHL, *J. Catal.* **21,** 282 (1971).
6. YU-YAO AND YUNG-FANG, *J. Catal.* **39,** 104 (1975).
7. R. P. RASTOGI, GURUDIP SINGH, B. L. DUBEY, AND C. S. SHUKLA, *J. Catal.* **65,** 25 (1980).
8. J. JENCK AND J. E. GERMAIN, *J. Catal.* **65,** 133 (1980).
9. SHINGO ANDO, *Coal Tar (Jap)* **7,** 525 (1955).
10. H. OHNISHI AND T. TERANISHI, *J. Phys. Soc. Japan* **16,** 35 (1961).
11. G. BLASSE, *Philips Res. Rep.* **18,** 383 (1963).
12. P. PORTA, F. S. STONE, AND R. G. TURNER, *J. Solid State Chem.* **11,** 135 (1974).
13. K. S. DE, J. GHOSE, AND K. S. R. C. MURTHY, *J. Solid State Chem.* **43,** 261 (1982).
14. (*a*) C. DELORME, *Compt. Rend.* **241,** 1588 (1955). (*b*) V. M. UST'YANTSEV AND V. P. MAR'EVICH, *Inorg. Mat.* **12,** 490 (1976).
15. T. M. YUREVA, G. K. BORESKOV, AND V. SH. GRUVER, *Kinet. Catal.* **12,** 116 (1971).
16. K. S. IRANI, A. P. B. SINHA, AND A. B. BISWAS, *J. Phys. Chem. Solids* **23,** 711 (1962).
17. J. B. GOODENOUGH, "Magnetism and the Chemical Bond," pp. 161, 210, Wiley, New York (1963).
18. A. NAVROTSKY AND O. J. KLEPPA, *J. Inorg. Nucl. Chem.* **29,** 2701 (1967).
19. J. D. DUNITZ AND L. E. ORGEL, *J. Phys. Chem. Solids* **3,** 20 (1957).
20. J. B. GOODENOUGH AND A. L. LOEB, *Phys. Rev.* **98,** 391 (1953).
21. M. D. STURGE, *Solid State Phys.* **20,** 149 (1967).
22. Y. OBI AND H. SAITO, *Phys. Status Solidi A* **16,** K9 (1973).
23. G. BLASSE, *Philips Res. Rep. Suppl.* 60 (1964).
24. S. T. KHIRSAGAR AND C. D. SABANE, *Japan J. Appl. Phys.* **10,** 794 (1971).
25. D. ADLER, *Solid State Phys.* **21,** 58 (1968).

26. A. K. BANERJEE, D. DUTTA, S. R. NAIDU, N. G. GANGULI, AND P. SEN, *Fertilizer Tech.* **12,** 299 (1975).
27. K. S. DE, J. GHOSE, AND K. S. R. C. MURTHY, *J. Thermal Anal.* **22,** 13 (1981).
28. J. D. STROUPE, *J. Amer. Chem. Soc.* **71,** 569 (1949).
29. A. NAVROSTSKY AND O. J. KLEPPA, *J. Inorg. Nucl. Chem.* **30,** 479 (1968).
30. F. MULLER AND O. J. KLEPPA, *J. Inorg. Nucl. Chem.* **35,** 2673 (1973).
31. E. PRINCE, *Acta Crystallogr.* **10,** 554 (1957).
32. E. PRINCE AND R. G. TREUTING, *Acta Crystallogr.* **9,** 1025 (1956).